NMR Studies of Defensin Antimicrobial Peptides. 1. Resonance Assignment and Secondary Structure Determination of Rabbit NP-2 and Human HNP-1†

Xiao-Lu Zhang,‡,§ Michael E. Selsted,‖ and Arthur Pardi*,⊥

Department of Chemistry and Biochemistry, University of Colorado at Boulder, Boulder, Colorado 80309-0215, Department of Pathology, University of California College of Medicine, Irvine, California 92717, and Department of Chemistry, Rutgers, The State University of New Jersey, New Brunswick, New Jersey 08903

Received May 21, 1992; Revised Manuscript Received August 22, 1992

ABSTRACT: Two-dimensional nuclear magnetic resonance spectroscopy has been used to make resonance assignments of the proton spectra of two defensin antimicrobial peptides, human neutrophil peptide HNP-1 and rabbit neutrophil peptide NP-2. The secondary structures of these peptides were determined from analysis of the proton–proton NOEs and from the positions of slowly exchanging amide protons. Both peptides contain a long stretch of a double-stranded antiparallel β-sheet in a hairpin conformation that contains a β-bulge, a short region of triple-stranded β-sheet, and several tight turns. The NMR results clearly show that HNP-1 forms a dimer or higher order aggregate in solution and that Pro^8 exists as a cis peptide bond. The NMR data on these peptides are compared with NMR data for a homologous peptide NP-5 [Bach, A. C., Selsted, M. E., & Pardi, A. (1987) *Biochemistry 26*, 4389–4397]. Analysis of the conformation-dependent proton chemical shifts shows that it is not possible to confidently judge the structural similarity of the three defensins from chemical shift data alone. However, comparison of the $^3J_{HN\alpha}$ coupling constants in NP-2 and NP-5 indicates that the backbone conformations for these peptides are very similar. A more detailed comparison of the solution conformations of the defensins peptides is made in the following paper in this issue where the NMR data are used as input for distance geometry and molecular dynamics calculations to determine the three-dimensional structures of HNP-1 and NP-2.

Neutrophils are phagocytic cells that play an active role in the mammalian defense system against foreign microbes (Hood et al., 1984). The defensins are a family of low molecular weight cationic peptides found in high concentrations (between 30% and 50% of the total protein) in the granules of certain neutrophils (Greenwald & Ganz, 1987; Lehrer et al., 1989) and have been shown to possess potent antimicrobial activity in vitro [see Lehrer et al. (1991) for a review]. These peptides employ an oxygen-independent mechanism for their activity, and it is thought that their mechanism of action involves membrane permeabilization (Lehrer et al., 1989; Kagan et al., 1990). Defensin peptides have been isolated from rat, guinea pig, rabbit, and human neutrophils, and the primary structures of 15 homologous peptides have been determined (Selsted et al., 1985a,b; Selsted & Harwig, 1987; Eisenhauer et al., 1989; Wilde et al., 1989). All the defensins contain three conserved disulfide linkages, one conserved arginine, and one conserved glycine residue. The defensins show potent in vitro microbicidal activity against Gram-positive and Gram-negative bacteria (Selsted et al., 1984; Ganz et al., 1985; Selsted & Harwig, 1987), fungi (Selsted et al., 1985c; Levitz et al., 1986; Segel et al., 1985), enveloped viruses (Daher et al., 1986; Lehrer et al., 1985; Selsted & Harwig, 1987), and mammalian tumor cells (Lichtenstein et al., 1986, 1988), with the spectrum and potency of the activity varying significantly among the individual peptides. To try to understand the molecular features that give rise to the different activities among these homologous peptides, we have used nuclear magnetic resonance spectroscopy to determine the structures of three defensin peptides that span the range and potencies of the defensin family. The solution structure of the rabbit peptide NP-5[1] has been previously determined (Pardi et al., 1988), and the X-ray crystal structure of the human defensin HNP-3 also has been recently determined (Hill et al., 1991). In this and the following paper (Pardi et al., 1992) the solution structures of the three peptides will be compared to each other and with the X-ray crystal structure.

MATERIALS AND METHODS

NMR Sample Preparation. The rabbit neutrophil peptide NP-2 and the human neutrophil peptide HNP-1 were isolated and purified as previously described (Ganz et al., 1985; Selsted et al., 1984). The NMR samples were prepared by dissolving 10 mg of NP-2 or 8 mg of HNP-1 in 0.4 mL of buffer consisting of 10 mM sodium phosphate, pH (or p^2H) 3.5. For the experiments in ^2H_2O, the sample was repeatedly dissolved in 99.8% ^2H_2O (Stohler Isotopes) and lyophilized with the final sample dissolved in 99.996% ^2H_2O (Stohler Isotope) under nitrogen. For the experiments in H_2O, the lyophilized sample

† This work was supported in part by funds from NIH Grants AI 22931 and AI 31696 to M.E.S. and by the Searle Scholars Program of the Chicago Community Trust (85-C110) and NIH Grant AI 27026 to A.P. A.P. is the recipient of a NIH Research Career Development Award 1991–1996 (AI 01051). The 400-MHz NMR spectrometer was purchased with partial support from NSF Grant CHEM-8300444, and the 500-MHz spectrometer was purchased with partial support from NIH Grant 4403283.

* Author to whom correspondence should be addressed.

‡ Rutgers.

§ Present address: Pharmaceuticals Division, Ciba-Geigy Corp., 556 Morris Ave., Summit, NJ 07901.

‖ University of California College of Medicine, Irvine.

⊥ University of Colorado at Boulder.

[1] Abbreviations: NP-5 rabbit neutrophil peptide 5; NP-2 rabbit neutrophil peptide 2; HNP-1, human neutrophil peptide 1; HNP-3, human neutrophil peptide 3; 2D, two dimensional; COSY, two-dimensional correlation spectroscopy; NOE, nuclear Overhauser effect; DQF-COSY, two-dimensional double-quantum filtered correlation spectroscopy; TOCSY, two-dimensional total correlation spectroscopy; FID, free induction decay; RELAYED-COSY, two-dimensional relayed coherence-transfer spectroscopy; t_1, evolution period; t_2, detection period; AMX, weakly coupled three-spin system.

0006-2960/92/0431-11348$03.00/0

was dissolved in 90% H_2O/10% ^2H_2O. For measurements of the slowly exchanging amide protons, samples were dissolved in 100% H_2O, lyophilized, and redissolved in 99.96% ^2H_2O, and a phase-sensitive COSY experiment (Marion & Wüthrich, 1983) was immediately performed.

NMR Experiments. The bulk of the NMR experiments were performed on a Varian XL-400 spectrometer operating at 400 MHz for protons, but some additional data were collected on a Varian VXR-500S spectrometer operating at 500 MHz. All 2D spectra were acquired in the phase-sensitive absorption mode with quadrature detection in both dimensions using the hypercomplex method (States et al., 1982). Generally 1024 or 2048 complex data points were collected during the acquisition time, t_2, 256–400 complex FIDs were collected during the evolution time, t_1, and a total of 48–96 transients were collected for each FID. The spectral width in both dimensions for the 400-MHz data was 4500 Hz except for the triple-quantum spectrum of NP-2, which had a spectral width of 6750 Hz in the t_1 dimension. Low-power irradiation of the residual water signal was applied during the recycle time (1.0–1.3 s) in the 2D spectra. The NMR data sets were transferred to a μVAX II or a Sun 4 computer and processed with the program FTNMR/FELIX (Hare Research, Inc.). The quadrature pair of FIDs for the first t_1 value in all 2D spectra was multiplied by 0.5 after Fourier transformation to eliminate t_1 ridge artifacts (Otting et al., 1986). For spectra taken in H_2O, a third-order polynomial baseline correction routine was applied to the amide region of the frequency domain spectrum after Fourier transformation in t_2 to eliminate modulation of the baseline caused by the tail of the residual water signal. For each spectrum both time domain signals were multiplied by a 0–90° phase-shifted sine bell matched filter window function and, if needed, then zero filled to 1024 or 2048 complex points before Fourier transformation. The COSY, RELAYED-COSY, DQF-COSY, triple-quantum spectroscopy, TOCSY, and 2D NOE experiments were performed using standard methods (Piantini et al., 1982; Eich et al., 1982; Braunschweiler & Ernst, 1983; Rance & Wright, 1986; Wüthrich, 1986). The TOCSY experiment employed a MLEV-16 pulse sequence for the spin lock (Davis & Bax, 1985). An 8.3-kHz radio frequency field was used for all pulses in the TOCSY experiment, and the spin lock pulse was applied for 54 ms with 3-ms trim pulses. The 2D NOE spectra were acquired with mixing times ranging from 50 to 200 ms. More detailed acquisition and processing parameters for each NMR experiment are given elsewhere (Zhang, 1989).

RESULTS

Sequential Resonance Assignment of NP-2. Resonance assignment of the proton spectrum of NP-2 was made by the sequential assignment procedure developed by Wüthrich (1986). This procedure starts by identification of protons belonging to the same spin system using a variety of 2D experiments that probe through-bond J-coupling connectivities. 2D NOE spectra in H_2O are then used to connect protons on neighboring residues which then provide the sequential connectivities.

Spin system identification was started using the DQF-COSY spectrum in ^2H_2O. Seven three-spin (AMX) systems were uniquely identified from the $C^\alpha H$–$C^\beta H$ and $C^\beta H$–$C^\beta H$ cross peaks. Figure 1 illustrates the connectivities for some of these spin systems. A triple-quantum spectrum was then used to confirm these assignments. In the triple-quantum spectrum, a three spin system, such as a $C^\alpha H$–$C^\beta H_2$ fragment, gives cross peaks at the triple-quantum frequency ($\delta_\alpha + \delta_{\beta 1} + \delta_{\beta 2}$)

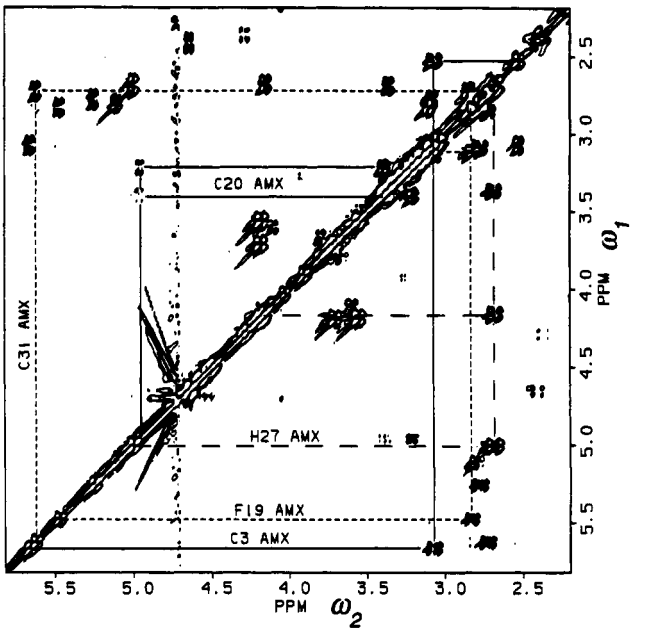

FIGURE 1: Contour plot of a DQF-COSY spectrum of NP-2 in ^2H_2O. The J-coupling connectivities for the AMX spin system of residues Cys^3, Phe^{19}, Cys^{20}, His^{27}, and Cys^{31} are illustrated. Both positive and negative contours are plotted.

in ω_1 and the single-quantum frequency of each spin in ω_2. This spectrum is extremely helpful in identifying three-spin systems when only two of the three spins can be identified in the single-quantum spectra due to spectral overlap. For example, the three-spin system for Cys^5 could not be identified in the DQF-COSY spectrum due to degeneracy of the two $C^\beta H$ chemical shifts; however, these shifts were readily extracted from the triple-quantum spectrum. Thus from the DQF-COSY and triple-quantum spectra, all three-spin, $C^\alpha H$–$C^\beta H_2$, systems consisting of six Cys, one Phe, and one His were unambiguously identified. In addition, sequence-specific assignments were made for Phe^{19} and His^{27} by observation of intraresidue NOEs from the aromatic ring protons to the C^α or C^β protons.

Many other non-AMX spin systems could not be unambiguously identified from the 2D spectra in ^2H_2O due to degeneracy of the chemical shifts of the C^α or side-chain protons. Therefore, resonance assignment proceeded by analysis of the amide proton connectivities in order to make use of the superior spectral resolution for this region of the spectrum. A COSY spectrum in H_2O was used to help make connections for an individual amide proton to its C^α proton(s). A RELAYED-COSY spectrum was used to connect an amide proton to its C^β proton(s), and the TOCSY spectrum allowed further extension of these connectivities to side-chain protons. When the information in the TOCSY and the DQF-COSY spectra in H_2O was combined, the following spin systems were uniquely identified: two Ile, two Val, two Pro, four Arg, and three Leu residues. Thus 26 of the 33 spin systems were identified at this point, and the remaining seven spin systems were subsequently identified during the sequential resonance assignment procedure.

The sequential resonance assignments were made by combining the COSY and 2D NOE spectra in H_2O, and Figure 2 shows such a plot where the $d_{\alpha N}$ (Wüthrich, 1986) connectivities for Pro^{12} to Gly^{24} are illustrated. The $d_{\alpha N}$ connectivites were observed for all amino acids in NP-2, except for the two prolines for which no such connectivities can be observed due to the absence of an amide proton. The $d_{\alpha N}$ connectivities, as well as the d_{NN} and $d_{\beta N}$ connectivities,

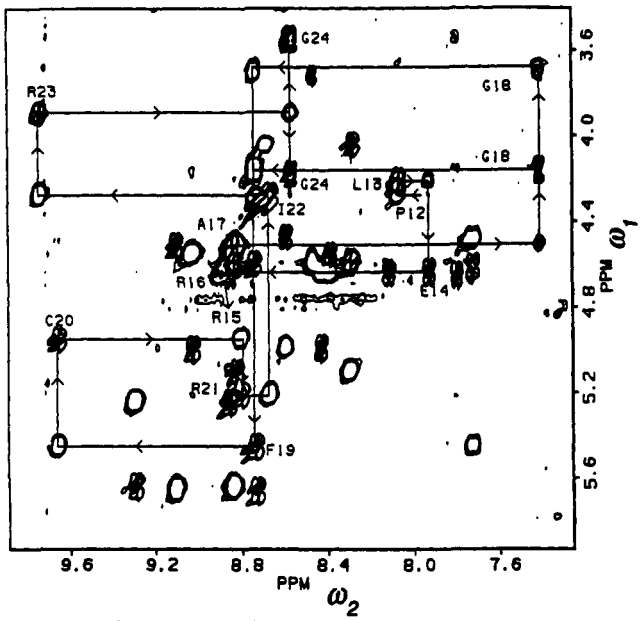

FIGURE 2: Contour plot of combined 2D NOE and COSY spectra of NP-2 in H_2O. The sequential resonance assignments are illustrated via $d_{\alpha N}$ connectivities for residues Pro[12]–Gly[24]. In the COSY spectrum, positive and negative contours are plotted, but only positive contours are plotted for the 2D NOE spectrum. The horizontal lines connect COSY and sequential 2D NOE cross peaks for the C^{α} protons, and the vertical lines connect sequential 2D NOE and COSY cross peaks for the amide protons. The arrows indicate the direction of the sequence.

Table I: Complete Sequential Connectivity Diagram for NP-2[a]

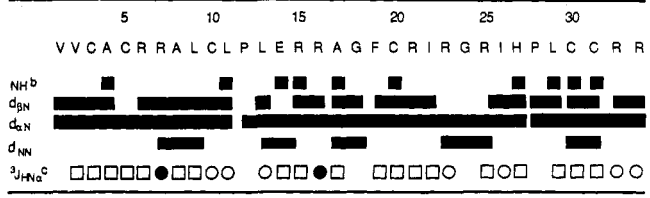

[a] The amino acid sequence of NP-2 is given using the standard single-letter abbreviations. [b] NH indicates which residues contain slowly exchanging amide protons. [c] ● indicates $^3J_{HN\alpha} < 6.0$ Hz, ○ indicates $6.0 \leq {}^3J_{HN\alpha} \leq 8.0$ Hz, and □ indicates $^3J_{HN\alpha} > 8.0$ Hz. The coupling constant could not be measured for the Gly, Pro, and N-terminal residues.

observed for NP-2 are shown in Table I. In summary, all backbone amide and C^{α} protons were assigned in NP-2, and all nonexchangeable side-chain protons for 24 of 33 residues were unambiguously assigned. The proton resonance assignments for NP-2 at 30 °C are listed in Table II.

Sequential Resonance Assignment of HNP-1. The sequential resonance assignment of HNP-1 proceeded in a manner similar to that described above for NP-2. Nearly complete resonance assignments of the proton spectrum of HNP-1 were made from analysis of five 2D NMR spectra: COSY and 2D NOE spectra in H_2O and DQF-COSY, 2D NOE, and TOCSY spectra in ^2H_2O. The proton spectrum of HNP-1 had less spectral overlap than NP-2, and so it was possible to identify all 30 amino acid spin systems from analysis of the DQF-COSY and TOCSY spectra in ^2H_2O. The residues Pro[8], Thr[19], and Leu[26] have unique spin systems in HNP-1 and therefore served as starting points in the sequential resonance assignment process. Figure 3 shows a plot of the combined 2D NOE and COSY spectra for HNP-1 in H_2O where the $d_{\alpha N}$ connectivities for Gly[18] to Cys[31] are illustrated. The sequential resonance assignments for HNP-1 could be made solely from the $d_{\alpha N}$ connectivities, and these assignments were generally confirmed by observation of $d_{\beta N}$ and/or d_{NN} connectivities (Wüthrich, 1986). The sequential connectivity diagram for HNP-1 is shown in Table III, and the only gaps in the sequential connectivities occurred for Pro[8] and Gly.[18] However, both these residues were uniquely assigned by $d_{\alpha N}$ connectivities with the next residue in the sequence. The amide and C^{α} protons for all residues, and all the nonexchangeable side-chain protons for 24 of the 30 residues, were unambiguously assigned in HNP-1, and the proton chemical shifts at 30 °C are given in Table IV.

Slowly Exchanging Amide Protons in NP-2 and HNP-1. The amide protons that exchange slowly (half lives greater than ≈5 h) were measured in NP-2 and HNP-1 by dissolving a lyophilized sample of peptide in 99.996% ^2H_2O and immediately recording a COSY spectrum. The residues that gave a NH–C^{α}H cross peak in the fingerprint region of the COSY spectrum were then identified as slowly exchanging and are listed for NP-2 and HNP-1 in Tables I and III, respectively.

Identification of Proton–Proton NOEs and Measurement of $^3J_{HN\alpha}$ Coupling Constants. The proton–proton NOEs in NP-2 and HNP-1 were measured from 2D NOE spectra at 200 ms. The NOE connectivities observed for NP-2 and HNP-1 are illustrated in the diagonal plots shown in Figure 4, panels a and b, respectively. A more detailed discussion of the observed NOEs and the distance constraints derived from 2D NOE spectra will be given in the following paper.

A high-resolution COSY spectrum in H_2O was used to measure the $^3J_{HN\alpha}$ coupling constants in NP-2 (Marion & Wüthrich, 1983). This COSY spectrum was acquired with 2048 complex points in t_2 and 450 complex FIDs in t_1. The data set was zero-filled to 4096 and 1024 complex points in t_2 and t_1, respectively, before Fourier transformation. The $^3J_{HN\alpha}$ coupling constants were measured from this spectrum (Marion & Wüthrich, 1983) for all residues in NP-2 (except for the N terminal and Gly and Pro residues) and are listed in Table I. The $^3J_{HN\alpha}$ coupling constants for HNP-1 could not be accurately measured due to the large (≥7 Hz) line widths for the amide protons in HNP-1.

DISCUSSION

Comparison of the Conformation-Dependent Chemical Shifts and the $^3J_{HN\alpha}$ Coupling Constants among Three Defensin Peptides. The chemical shifts of the proton resonances in proteins are very dependent upon the primary, secondary, and tertiary structure of the molecule, and thus proton chemical shifts potentially contain a great deal of structural information (Wüthrich, 1986). Correlations have been found between proton chemical shifts and ring current effects from the aromatic residues in proteins (Perkins & Wüthrich, 1979) or hydrogen-bond lengths (Pardi et al., 1983; Wagner et al., 1983). The conformation-dependent chemical shifts of the backbone amide and C^{α} protons have been calculated for the two peptides studied here, NP-2 and HNP-1, as well as for the rabbit peptide NP-5 (Bach et al., 1987). These conformation-dependent chemical shifts were calculated by subtracting the "random coil" chemical shifts (Wüthrich, 1986) from the observed chemical shifts for each amino acid residue in the three peptides. Thus these residual conformation-dependent chemical shifts should be, on the average, independent of the primary structure and therefore reflect higher order structure of the peptides.

It would be extremely valuable to be able to qualitatively determine the conformational similarity among several proteins by simple comparison of chemical shifts, and there are several

Table II: ^{1}H Chemical Shifts (ppm) for the Assigned Proton Resonances of NP-2 at 30 °C in 10 mM Sodium Phosphate, pH 3.5[a]

residue	NH	C$^\alpha$H	C$^\beta$H	others
Val^1		4.06	2.15	C$^\gamma$H$_3$, 1.00, 1.00
Val^2	8.68	4.31	1.92	C$^\gamma$H$_3$ 0.95, 0.91
Cys^3	8.71	5.66	3.07, 2.52	
Ala^4	9.09	4.51	1.21	
Cys^5	8.79	5.10	2.79, 2.79	
Arg^6	8.28	4.58	1.55	C$^\beta$H/C$_\gamma$H$_2$[b] 1.77
Arg^7	8.46	3.72	1.84	C$^\beta$H/C$^\gamma$H$_2$[b] 1.62, 1.50; C$^\delta$H$_2$ 3.18; N$^\epsilon$H 7.24
Ala^8	8.72	4.59	1.41	
Leu^9	8.11	4.64	1.64	C$^\gamma$H 1.61; C$^\delta$H$_3$ 0.91, 0.91
Cys^{10}	8.42	4.99	3.37, 2.69	
Leu^{11}	8.58	4.48	1.68, 1.25	C$^\gamma$H 1.57; C$^\delta$H$_3$ 0.86, 0.86
Pro^{12}		4.28	2.36, 1.81	C$^\gamma$H$_2$ 2.11, 2.00; C$^\delta$H$_2$ 3.79, 3.66
Leu^{13}	8.07	4.21	1.91, 1.66	C$^\gamma$H 1.57; C$^\delta$H$_3$ 0.86, 0.86
Glu^{14}	7.92	4.64	2.40	C$^\beta$H/C$^\gamma$H$_2$[b] 2.09, 1.82, 1.55
Arg^{15}	8.84	4.66	1.68	C$^\gamma$H$_2$ 1.48; C$^\delta$H$_2$ 3.14; N$^\epsilon$H 7.26
Arg^{16}	8.89	4.67	1.95	C$^\beta$H/C$^\gamma$H[b] 1.85, 1.57; C$^\gamma$H 1.72; C$^\delta$H$_2$ 3.11, 3.22; N$^\epsilon$H 7.17
Ala^{17}	8.84	4.52	1.21	
Gly^{18}	7.40	4.17, 3.68		
Phe^{19}	8.73	5.45	3.08, 2.82	ring: C3H, C5H 7.25; C2H, C6H 7.12
Cys^{20}	9.64	4.95	3.38, 3.23	
Arg^{21}	8.80	5.21	1.60, 1.36	C$^\gamma$H$_2$ 1.40, 1.32; C$^\delta$H$_2$ 3.05; N$^\epsilon$H 7.20
Ile^{22}	8.66	4.27	1.49	C$^\gamma$H$_2$ 1.39, 1.04; C$^\gamma$H$_3$ 0.82; C$^\delta$H$_3$ 0.51
Arg^{23}	9.73	3.90	2.04, 1.80	C$^\gamma$H$_2$ 1.66, 1.62; C$^\delta$H$_2$ 3.24, 3.20; N$^\epsilon$H 7.22
Gly^{24}	8.56	4.18, 3.54		
Arg^{25}	7.79	4.65	1.83, 1.78	C$^\gamma$H$_2$ 1.69, 1.57; C$^\delta$H$_2$ 3.22
Ile^{26}	8.38	4.55	1.61	C$^\gamma$H$_2$ 1.30, 0.96; C$^\gamma$H$_3$ 0.68; C$^\delta$H$_3$ 0.49
His^{27}	9.02	5.00	4.16, 2.65	ring: C2H 8.76; C4H 7.06
Pro^{28}		4.49	1.99, 1.80	C$^\gamma$H$_2$ 1.97, 1.75; C$^\delta$H$_2$ 4.10, 3.59
Leu^{29}	7.71	4.62	1.32, 0.84	C$^\gamma$H 1.16; C$^\delta$H$_3$ 0.70, 0.64
Cys^{30}	8.84	5.24	3.05, 2.76	
Cys^{31}	9.29	5.64	2.84, 2.73	
Arg^{32}	8.82	4.58	1.89	C$^\beta$H/C$^\gamma$H$_2$[b] 1.75
Arg^{33}	8.27	4.05	1.78, 1.69	C$^\gamma$H$_2$ 1.59, 1.57; C$^\delta$H$_2$ 3.14; N$^\epsilon$H 7.10

[a] The chemical shifts are referenced to the H_2O or HOD resonance at 4.70 ppm. The chemical shifts have errors of ±0.02 ppm. Only assigned protons are listed. [b] Not specifically assigned to C$^\beta$H or C$^\gamma$H.

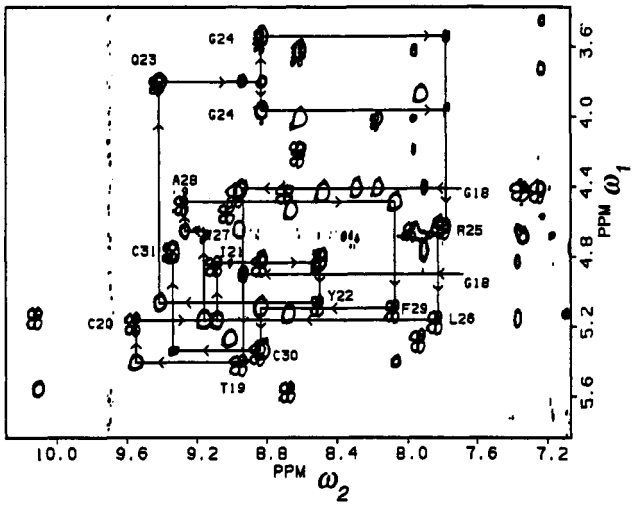

FIGURE 3: Contour plot of a combined 2D NOE and COSY spectrum of HNP-1 in H_2O. The sequential resonance assignments are illustrated via $d_{\alpha N}$ connectivities for residues Gly^{18} to Cys^{31}. The format of the plot is the same as that described in the legend to Figure 2.

Table III: Complete Sequential Connectivity Diagram for HNP-1[a]

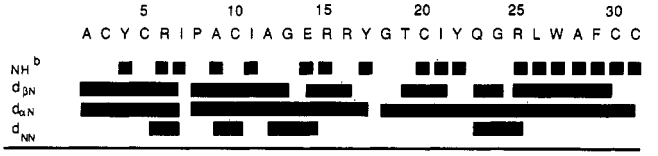

[a] The amino acid sequence of HNP-1 is given using the standard single-letter abbreviations. [b] NH indicates which residues contain slowly exchanging amide protons.

recent reports of correlations between secondary structure and ^{1}H chemical shifts in proteins (Williamson, 1990; Wishart et al., 1991). The three defensin peptides have a reasonably high degree of sequence identity (11 out of 30 amino acids) so it is of interest to see how well the conformation-dependent chemical shifts correlate in these homologous peptides. Figure 5 panels a and b show the conformation-dependent chemical shifts for the amide and C$^\alpha$ protons, respectively, for NP-2, NP-5, and HNP-1. The plots show significant variation of the conformation-dependent chemical shifts among the three peptides with the correlations coefficients among the three peptides ranging from 0.62 to 0.66 for the amide protons and 0.48 to 0.88 for the C$^\alpha$ protons. For comparison, the correlation coefficient for the amide proton chemicals shifts for NP-2 and NP-5 is <0.2 when the order of the amino acids is randomly scrambled. One factor that may contribute to these relatively low correlation coefficients is the different ring current effects experienced by amide or C$^\alpha$ protons in the different peptides. For example, the largest variation in the conformation-dependent chemical shifts of the amide proton occurs for residue 6, where HNP-1 has a shift 1.1 ppm greater than either NP-2 or NP-5. However, HNP-1 has a tryptophan at residue 27 instead of the histidine in NP-2 and NP-5; this tryptophan appears to exert a much larger ring current effect for the backbone and side-chain protons on Arg^6 and Ile^7 as compared with the ring current shifts for these residues in NP-2 and NP-5. Another factor that could contribute to the variations in the conformation-dependent chemical shifts is different extents (or kinetics) for dimer formation or aggregation in the three peptides. As will be discussed below, we have only qualitative NMR evidence for formation of higher order complexes and therefore cannot compare the concen-

Table IV: ^{1}H Chemical Shifts (ppm) for the Assigned Proton Resonances of HNP-1 at 30 °C in 10 mM Sodium Phosphate, pH 3.5[a]

residue	NH	C$^\alpha$H	C$^\beta$H	others
Ala^2		3.93	1.35	
Cys^3	7.97	5.33	2.42, 1.66	
Tyr^4	9.06	4.58	2.91, 2.26	ring: C2H, C6H 6.96; C3H, C5H 6.65
Cys^5	8.71	5.62	2.29	
Arg^6	10.16	5.17	1.70	C$^\gamma$H$_2$ 1.72, 1.46; C$^\delta$H$_2$ 3.23, 3.19
Ile^7	8.73	4.47	1.15	C$^\gamma$H$_3$ 0.52; C$^\gamma$H$_2$ 1.12, 0.73; C$^\delta$H$_3$ –0.47
Pro^8		4.63	2.27, 2.16	C$^\gamma$H$_2$ 2.01, 1.78; C$^\delta$H$_2$ 3.78, 3.50
Ala^9	7.28	4.47	1.41	
Cys^{10}	8.34	4.75	3.40, 2.56	
Ile^{11}	7.38	4.45	1.90	C$^\gamma$H$_3$ 0.85; C$^\gamma$H$_2$ 1.14, 0.86; C$^\delta$H$_3$ 0.72
Ala^{12}	8.22	4.06	1.35	
Gly^{13}	8.66	4.24, 3.67		
Glu^{14}	8.01	4.68	2.44, 2.22	C$^\gamma$H 1.74
Arg^{15}	9.01	4.48	1.55	C$^\gamma$H$_2$ 1.55, 1.41; C$^\delta$H 3.11
Arg^{16}	8.54	4.85	1.95	C$^\gamma$H$_2$ 1.95, 1.89; C$^\delta$H$_2$ 3.33, 3.27
Tyr^{17}	8.87	4.88	2.89, 2.66	ring: C2H, C6H 7.10; C3H, C5H 6.80
Gly^{18}	7.95	4.96, 4.46		
Thr^{19}	8.99	5.46	3.85	C$^\gamma$H$_3$ 1.30
Cys^{20}	9.60	5.21	3.06, 2.32	
Ile^{21}	9.14	4.90	1.81	C$^\gamma$H$_3$ 0.90; C$^\gamma$H$_2$ 1.39, 0.97; C$^\delta$H$_3$ 0.75
Tyr^{22}	8.54	5.10	2.91, 2.17	ring: C2H, C6H 6.54; C3H, C5H 6.46
Gln^{23}	9.46	3.85	2.21, 1.95	C$^\gamma$H$_2$ 1.83, 1.30
Gly^{24}	8.87	4.02, 3.60		
Arg^{25}	7.82	4.67	1.59	C$^\gamma$H$_2$ 1.57, 1.45; C$^\delta$H$_2$ 2.89, 2.84
Leu^{26}	7.87	5.21	1.62, 1.35	C$^\gamma$H 1.54; C$^\delta$H$_3$ 0.81, 0.78
Trp^{27}	9.21	4.71	3.40, 2.74	ring: N1H 10.18; C2H 7.40; C4H 7.06; C5H 7.12; C7H 7.17
Ala^{28}	9.32	4.54	1.34	
Phe^{29}	8.12	5.16	2.68, 2.51	ring: C2H, C6H 6.62; C3H, C5H 6.23
Cys^{30}	8.88	5.39	2.96, 2.75	
Cys^{31}	9.40	4.81	3.37, 2.53	

[a] The chemical shifts are referenced to the H_2O or HOD resonance at 4.70 ppm. The chemical shifts have errors of ±0.02 ppm. Only assigned protons are listed.

trations of the various species in the three defensins. Thus, from simple comparison of the conformation-dependent chemical shifts, it is not possible to confidently judge the similarity of the structures for these homologous peptides.

Figure 6 shows a correlation plot of the $^3J_{HN\alpha}$ coupling constants for the rabbit peptides NP-2 and NP-5 [the couplings for NP-5 were taken from Bach et al. (1987)]. The correlation of these backbone J couplings is generally much better than the conformation-dependent chemical shifts with a correlation coefficient of 0.79 (for comparison, the correlation coefficient is <0.15 with a random order of the measured J couplings). Since the $^3J_{HN\alpha}$ couplings constants contain information on the backbone torsion angle ϕ through a Karplus-type relation (Pardi et al., 1984), these data qualitatively indicate that NP-2 and NP-5 possess similar backbone conformations. Unfortunately, it was not possible to make analogous comparisons for HNP-1 since the large line widths for this peptide prevented accurate measurement of the $^3J_{HN\alpha}$ coupling constants. Thus, the $^3J_{HN\alpha}$ coupling constants provide a more useful criteria than ^{1}H chemical shifts for qualitative comparison of the structure of the defensins.

Identification of Secondary Structure in NP-2. Regular secondary structure in proteins can often be derived from qualitative inspection of the NOEs between backbone protons in the 2D NOE spectrum (Wüthrich, 1986). The observed NOE connectivities between protons in NP-2 are shown in the diagonal plot in Figure 4a. This plot shows no evidence for any α-helical secondary structure in NP-2. Previous studies have shown that helical regions can also be reliably identified by a string of three or more sequential amino acids having $^3J_{HN\alpha}$ coupling constants ≤6 Hz (Pardi et al., 1984), and, as seen in Table I, no such pattern is observed in NP-2. Thus it is clear that there are no stable α-helical regions in NP-2.

The diagonal plot in Figure 4a also shows a string of NOEs running perpendicular to the diagonal and contacting the diagonal around residue 24. This indicates the presence of an antiparallel β-sheet in a hairpin geometry with a turn at residues 22–25. This secondary structure is similar to the β-hairpin previously observed in the homologous peptide NP-5 (Pardi et al., 1988). Some of the most distinctive indicators of the antiparallel β-sheet in NP-2 are the C$^\alpha$H–C$^\alpha$H NOEs between residues on opposite strands (Wüthrich, 1986), and such interactions are seen for Arg^{21}–Ile^{26}, Phe^{19}–Pro^{28}, and Arg^{16}–Cys^{30}. These NOE connectivities are consistent with an antiparallel β-sheet extending from at least Arg^{16} to Cys^{30}. These and other indicators of this antiparallel β-sheet are illustrated in Figure 7A where the slowly exchanging amide protons and NOE connectivities between backbone amide or C$^\alpha$ protons for residues in the β-sheet are shown. There are additional cross-strand NOE connectivities involving amide and C$^\alpha$ protons for residues Gly^{18}–Leu^{29}. However, the pattern of the cross-strand connectivities and slowly exchanging amide protons for residues 16–18 and 30 is not consistent with a standard antiparallel β-sheet. A β-bulge was observed by Eisenberg and co-workers in their crystal structure of a dimer of the human defensin HNP-3 (Hill et al., 1991), and the NMR data also show the presence of a β-bulge for residue Gly^{18}. This evidence includes: (i) A cross-strand NOE between the C$^\alpha$H on Cys^{30} and the C$^\alpha$H on Arg^{16} instead of the C$^\alpha$H residue Ala^{17}, which is the NOE predicted for a standard antiparallel β-sheet. (ii) The NH of Ala^{17}, but not the NH for Gly^{18}, is slowly exchanging, which is consistent with a structure where the Ala^{17} amide proton (not the Gly^{18} amide proton) is involved in a cross-strand hydrogen bond with the carbonyl oxygen of Pro^{28}. The amide proton on residue 31 is slowly exchanging (see Table I) and may form a cross-strand hydrogen bond with the carbonyl of Arg^{15}, which would be consistent with the β-sheet structure extending from residue 15 to 31. Gly^{18} is conserved in all the defensin peptides sequenced to data, and thus, as pointed out by Hill et al.

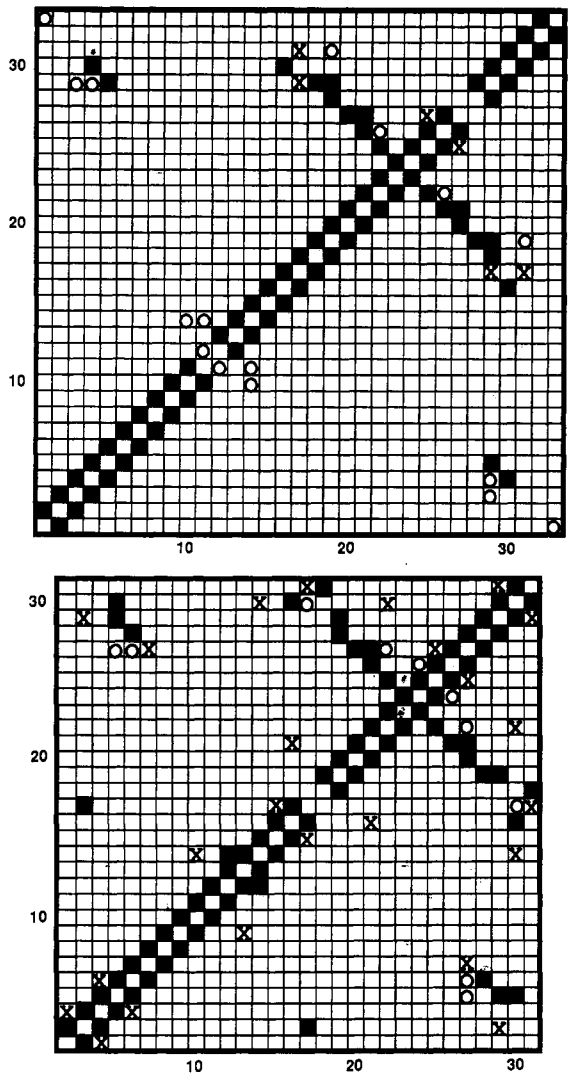

FIGURE 4: Diagonal plot of the observed NOEs in (a, top) NP-2 and (b, bottom) HNP-1. The axes correspond to the amino acid residue numbers. The filled squares indicate NOEs between backbone protons, the circles indicate NOEs between backbone and side-chain protons, and the crosses indicate NOEs between side-chain protons. Where a filled square and a circle or cross occupy the same location, only the square is shown; and if a circle and a cross occupy the same location, only the circle is shown.

(1991), it may be the only residue that can be accommodated in this β-bulge structure.

There is also evidence for an additional short stretch of antiparallel β-sheet in NP-2. As seen in the diagonal plot in Figure 4a, there are several NOEs between backbone protons on residues 4–5 and 29–30. Specifically, NOEs were observed between amide protons on Ala^4 and Cys^{30} and the C$^\alpha$ protons on Cys^5 and Leu^{29}. This pattern of cross-strand NOEs, along with the disulfide linkage between residues Cys^3 and Cys^{31}, is consistent with an antiparallel β-sheet structure for this region of the peptide. In addition to the cross-strand NOEs observed at 400 MHz, an additional C$^\alpha$H–C$^\alpha$H NOE was observed between Cys^3 and Cys^{31} from NOE data collected at 500 MHz. The similar chemical shifts for these resonances (see Table II) led to this cross peak being too close to the diagonal to observe at lower field, but it was readily observed at 500 MHz (data not shown). Figure 7A shows the NMR evidence for a short region of antiparallel β-sheet involving residues 3–6 and 28–31, and, as seen in the figure, the amide protons for residues 30 and 4 are slowly exchanging in NP-2, which is again consistent with this antiparallel β-sheet. These

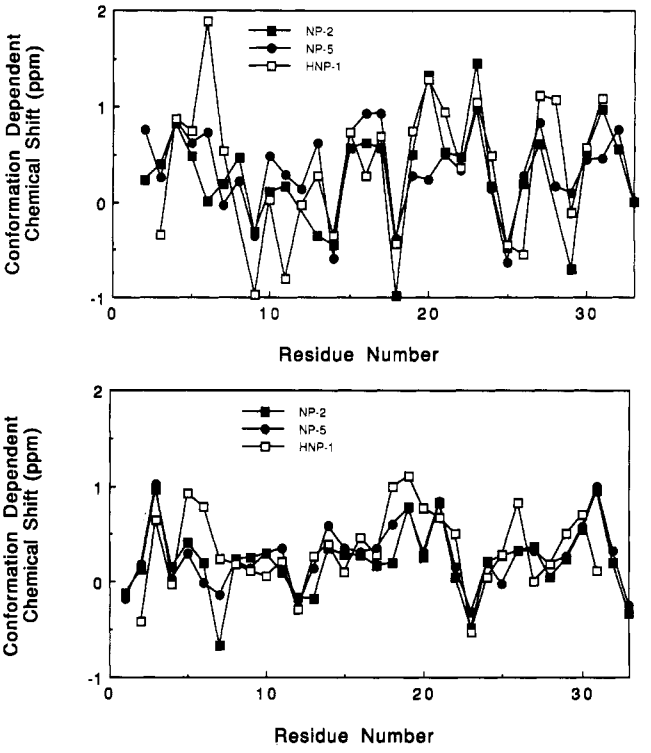

FIGURE 5: (a, top) Conformation-dependent chemical shifts versus amino acid residue number for the amide protons in NP-2, HNP-1, and NP-5. (b, bottom) Conformation-dependent chemical shifts versus amino acid residue number for the C$^\alpha$ protons in NP-2, HNP-1, and NP-5. The conformation-dependent chemical shifts were calculated by subtracting the "random coil" chemical shifts as discussed in the text. The filled squares correspond to NP-2, the filled circles to NP-5, and the open squares to HNP-1.

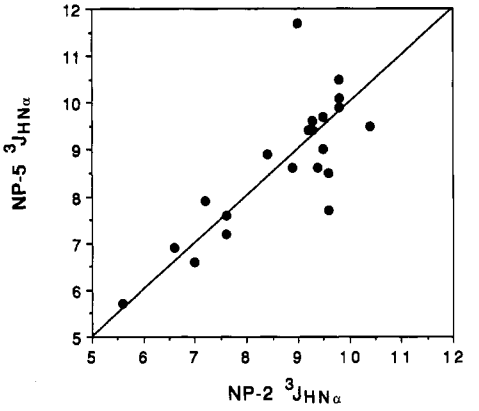

FIGURE 6: Correlation plot of the experimental $^3J_{HN\alpha}$ coupling constants for NP-2 and NP-5.

results indicate a short region of triple-stranded β-sheet in NP-2, and, as will be discussed below, the NMR data for HNP-1 also show strong evidence for this β-sheet secondary structure in this region.

Qualitative analysis of the proton–proton NOEs and $^3J_{HN\alpha}$ coupling constants in a peptide can be used to identify tight turns in proteins and peptides (Wüthrich, 1986). One of the criteria for identification of β-turns is NOE(s) between backbone protons on residues i and i+2 or i+3. Only one such NOE was unambiguously assigned in NP-2, which was an NOE between amide protons on residues 22 and 25 that are involved in the turn of the β-hairpin secondary structure in the peptide. Strong sequential d_{NN} cross peaks between residues 23–24 and 24–25 are most consistent with a classical type I or I′, and the $^3J_{HN\alpha}$ coupling constant of 7.0 Hz for

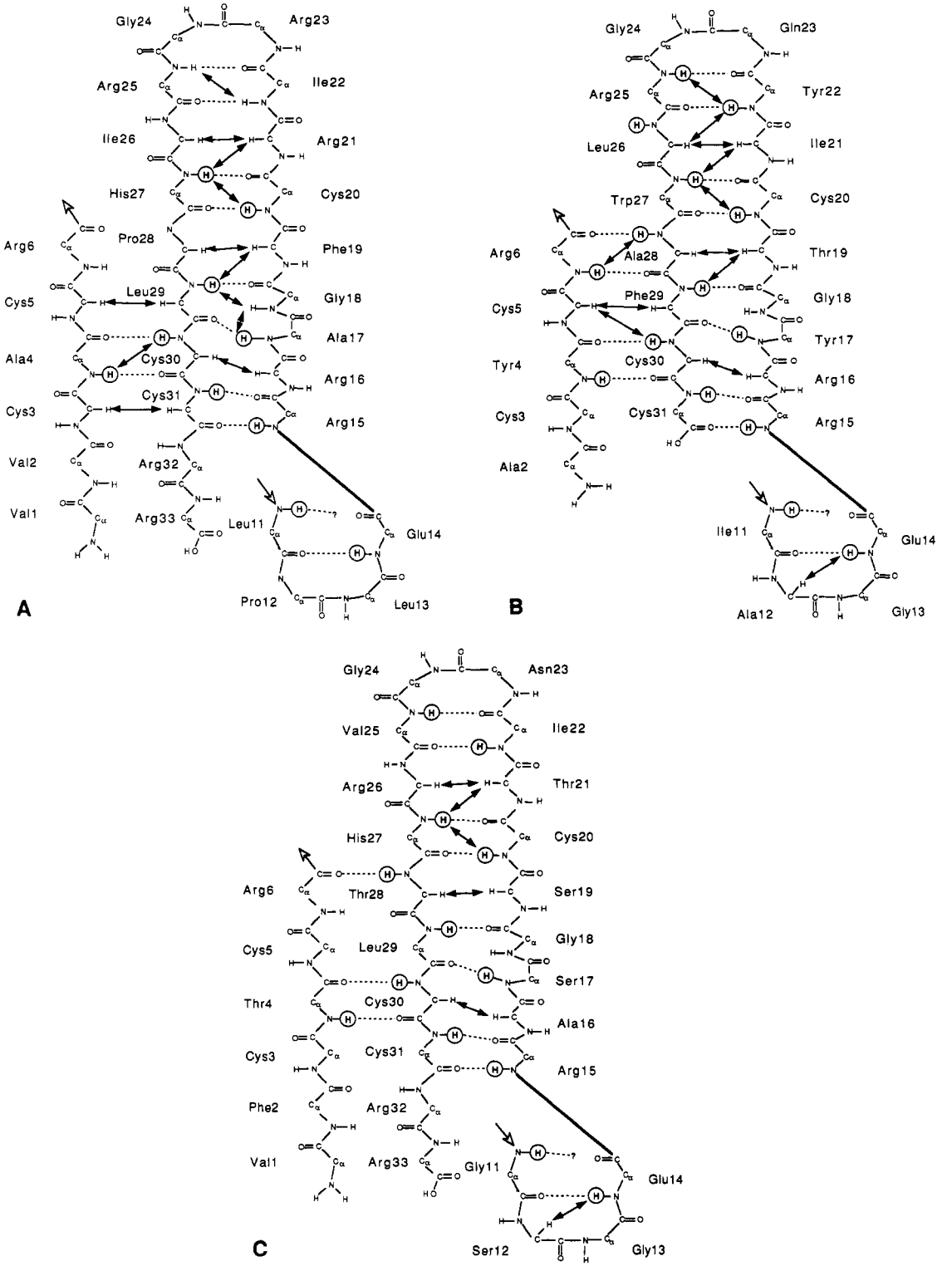

FIGURE 7: Schematic representation of the secondary structure of (A) NP-2, (B) HNP-1, and (C) NP-5. Backbone proton–backbone proton NOEs are indicated by the double-headed arrows, and the slowly exchanging amide protons are circled. Dashed lines indicate putative hydrogen-bonding interactions. The interactions for the loop region from residues 7 to 11 are not shown.

residue 23 suggests a type I′ turn. However, from this pattern recognition procedure, it is not possible to unambiguously identify any other tight turns in NP-2.

Identification of Secondary Structure in HNP-1. A procedure similar to that describe above was used to identify secondary structure in HNP-1. The long stretch of antiparallel β-sheet in a hairpin configuration is clearly observed in the diagonal plot of HNP-1 shown in Figure 4b. The NOE connectivity patterns and the slowly exchanging amide protons in HNP-1 are again consistent with a β-sheet involving residues 15–31 with a β-bulge for Gly[18] as shown in Figure 7B. There is also strong evidence for a short stretch of triple-stranded β-sheet involving residues 3–6. A cross-strand NOE is observed between amide protons on residues Arg[6] and Ala[28], and both these amide protons are also found to be slowly exchanging, which is consistent with the antiparallel β-sheet extending to include these residues. However, the use of slowly exchanging amide protons to help identify or confirm secondary structure in HNP-1 is somewhat limited due to the intermolecular aggregation of the peptide (discussed below), which

leads to many more slowly exchanging amide protons in HNP-1 as compared with NP-2 or NP-5.

The evidence for tight turns in HNP-1 is generally less reliable due to the fact that accurate $^3J_{HN\alpha}$ coupling constant could not be measured. However, the presence of a β-sheet in a hairpin conformation indicates a tight turn for residues 22–25. The observation of d_{NN} connectivities between residues 23–24 and 24–25 indicates the presence of a type I or I′ turn; however, no further distinction can be made from the backbone NOE data. Another tight turn involving residues Ile[11]–Glu[14] was identified in HNP-1 from the following data: a $d_{\alpha N}(i,i+2)$ connectivity between residues Ala[12] and Glu[14], sequential d_{NN} connectivities for residues Ala[12]–Gly[13] and Gly[13]–Glu[14], and a slowly exchanging amide proton for Ile[11] (Wüthrich, 1986). These data indicate a type I or I′ turn, but again no further distinction can be made from these data.

Cis Peptide Bond for Pro[8] in HNP-1. The cis–trans isomerization of proline residues plays an important role in the folding and unfolding of many proteins (Creighton, 1984). In a trans peptide bond, the shortest distance between neighboring C^α protons is 4.2 Å, so these sequential NOEs are generally not observed (Wüthrich, 1986). However, for a cis peptide bond, the distance between neighboring C^α protons can be as short as 2.1 Å so a cis peptide bond is readily identified by observation of a short $d_{\alpha\alpha}$ connectivity. A short $d_{\alpha\alpha}$ connectivity between residues Ile[7] and Pro[8] was observed in the 2D NOE spectrum of HNP-1, indicating the presence of a *cis*-proline. Analysis of the 2D NMR experiments on HNP-1 shows no evidence of a significant population of trans isomer for Pro[8] in HNP-1, and thus this residue exists predominantly in a single conformation in solution.

NMR Evidence for Molecular Aggregation of HNP-1. As previously mentioned, HNP-1 shows 18 slowly exchanging amide proton whereas NP-2 and NP-5 show only 9 and 10 slowly exchanging amide protons, respectively. It is somewhat surprising to find such a large difference in the number of slowly exchanging amide protons in these homologous peptides. The amide proton exchange rates are slowed when the protons are involved in intramolecular hydrogen bonding or when the protons are buried on the interior of the protein and have low solvent-accessible surface areas (Lee & Richards, 1971; Wagner & Wüthrich, 1982). A large percentage of the amide protons are slowly exchanging in HNP-1 because the peptide appears to form an intermolecular complex; thus many of the amide protons may be less accessible to solvent in HNP-1 than in NP-2 or NP-5. Other NMR evidence also supports formation of an intermolecular complex in HNP-1. First, the average proton line widths in HNP-1 are significantly larger than those observed in NP-2 or NP-5 (data not shown). This complex formation leads to lower signal-to-noise ratios for cross peaks in COSY-type spectra, or triple-quantum spectra on HNP-1, and higher signal-to-noise ratios for cross peaks in the 2D NOE spectra, as compared to the other peptides. As noted earlier, the larger line widths for HNP-1 made it difficult to accurately measure the $^3J_{HN\alpha}$ coupling constants. These HNP-1 NMR data are consistent with molecular aggregation of the peptide leading to a longer rotational correlation time for this peptide as compared with NP-2 or NP-5.

Comparison of the Secondary Structure in the Three Defensins. A more extensive comparison of the three-dimensional structures of the three defensins is made in the following paper (Pardi et al., 1992); however, comparison of the diagonal plots [Figure 4a,b and Figure 1 in Pardi et al. (1988)] and the secondary structure diagrams in Figure 7 indicate that the three homologous peptides have similar global structure. One difference between these peptides was the lack of backbone–backbone NOEs for the third strand of β-sheet in NP-5 as compared with the other two peptides. As seen in Figure 7, no such NOEs were observed in NP-5; however, NP-2 and HNP-1 contain 2 and 3, respectively, cross-strand NOEs between residues 3–6 and 28–30. This absence of NOEs in NP-5 precluded the unambiguous identification of the short region of triple-stranded sheet in this peptide. All three peptides have varying degrees of evidence for the formation of a β-bulge at residue 18. As discussed above, the strongest evidence for this is in NP-2 where the amide proton on Gly[18] shows a cross-strand NOE to the amide proton on Leu[29]. This distance is too long to observe in a standard β-sheet. This interaction could not be unambiguously assigned in HNP-1 due to limited spectral resolution and was not observed in NP-5. However, a strong $C^\alpha H$–$C^\alpha H$ NOE was observed between residues 16 and 30 in all three peptides, which is again consistent with the formation of the β-bulge at residue 18.

The hydrogen exchange properties differ significantly in the three peptides, with HNP-1 having many more slowly exchanging amide protons than NP-2 or HNP-1. As seen in Figure 7B, most of these protons are in secondary structure regions where the amide protons could readily form intramolecular hydrogen bonds. However, the two slowly exchanging amide protons on residues 21 and 26 are on the exterior of the β-hairpin and from the three-dimensional structures (Pardi et al., 1988, 1992; Hill et al., 1991) should not be involved in any intramolecular hydrogen-bonding interactions. As will be more extensively discussed in the following paper, these data help to confirm that HNP-1 is not a monomer under the conditions observed here.

In conclusion, the solution NMR properties of the three defensins, NP-2 and HNP-1 studied here and the previously determined structures for NP-5 (Pardi et al., 1988), show that these antimicrobial peptides have similar secondary structures. The proton–proton NOEs provide the primary evidence showing similar structures for these defensins. In addition, comparison of the $^3J_{HN\alpha}$ coupling constants in NP-2 and NP-5 indicate that the backbone conformations of these peptides are very similar. However, from comparison of the proton chemical shifts alone, it is not possible to confidently judge the similarity of the defensin structures. The differences observed in the conformation-dependent chemical shifts of the three defensins could arise from different ring current effects (caused by different primary structures) or could result from subtle differences in the local structure of the peptides. HNP-1 shows very different hydrogen exchange properties with many more slowly exchanging amide protons than NP-2 or NP-5. These data combined with the larger line widths observed for HNP-1 relative to NP-2 or NP-5 indicate that HNP-1 exists as a dimer or higher order aggregate in solution. A more detailed comparison of the conformation for the three defensins is given in the following paper (Pardi et al., 1992).

REFERENCES

Bach, A. C., Selsted, M. E., & Pardi, A. (1987) *Biochemistry 26*, 4389–4397.

Braunschweiler, L., & Ernst, R. R. (1983) *J. Magn. Reson. 53*, 521–528.

Creighton, T. E. (1984) *Proteins, Structures and Molecular Principles*, Freeman & Co., New York.

Daher, K. A., Selsted, M. E., & Lehrer, R. I. (1986) *J. Virol. 60*, 1068–1074.

Davis, D. G., & Bax, A. (1985) *J. Am. Chem. Soc. 107*, 2820–2821.

Eich, G., Bodenhausen, G., & Ernst, R. R. (1982) *J. Am. Chem. Soc. 104*, 3731–3732.
Eisenhauer, P. B., Harwig, S. S., Szklarek, D., Ganz, T., Selsted, M. E., & Lehrer, R. I. (1989) *Infect. Immun. 57*, 2021–2027.
Ganz, T., Selsted, M. E., Szklarek, D., Harwig, S. S., Daher, K., Bainton, D. F., & Lehrer, R. I. (1985) *J. Clin. Invest. 76*, 1427–1435.
Greenwald, G. I., & Ganz, T. (1987) *Infect. Immun. 55*, 1365–1368.
Hill, C. P., Yee, J., Selsted, M. E., & Eisenberg, D. (1991) *Science 251*, 1481–1485.
Hood, L. E., Weissman, I. L., Wood, W. B., & Wilson, J. H. (1984) *Immunology*, Benjamin Cummings Inc., Menlo Park, CA.
Kagan, B. L., Selsted, M. E., Ganz, T., & Lehrer, R. I. (1990) *Proc. Natl. Acad. Sci. U.S.A. 87*, 210–214.
Lee, B., & Richards, F. M. (1971) *J. Mol. Biol. 55*, 379–400.
Lehrer, R. I., Daher, K., Ganz, T., & Selsted, M. E. (1985) *J. Virol. 54*, 467–472.
Lehrer, R. I., Barton, A., Daher, K. A., Harwig, S. S., Ganz, T., & Selsted, M. E. (1989) *J. Clin. Invest. 84*, 553–561.
Lehrer, R. I., Ganz, T., & Selsted, M. E. (1991) *Cell 64*, 229–230.
Levitz, S. M., Selsted, M. E., Ganz, T., Lehrer, R. I., & Diamond, R. D. (1986) *J. Infect. Dis. 154*, 483–489.
Lichtenstein, A., Ganz, T., Selsted, M. E., & Lehrer, R. I. (1986) *Blood 68*, 1407–1410.
Lichtenstein, A. K., Ganz, T., Nguyen, T. M., Selsted, M. E., & Lehrer, R. I. (1988) *J. Immunol. 140*, 2686–2694.
Marion D., & Wüthrich, K. (1983) *Biochem. Biophys. Res. Commun. 113*, 967–974.
Otting, G., Widmer, H., Wagner, G., & Wüthrich, K. (1986) *J. Magn. Reson. 66*, 187–193.
Pardi, A., Wagner, G., & Wüthrich, K. (1983) *Eur. J. Biochem. 137*, 445–454.
Pardi, A., Billeter, M., & Wüthrich, K. (1984) *J. Mol. Biol. 180*, 741–751.
Pardi, A., Hare, D. R., Selsted, M. E., Morrison, R. D., Bassolino, D. A., & Bach, A. C. I. (1988) *J. Mol. Biol. 201*, 625–636.
Pardi, A., Zhang, X.-L., Selsted, M. E., Skalicky, J. J., & Yip, P. F. (1992) *Biochemistry* (following paper in this issue).
Perkins, S. J., & Wüthrich, K. (1979) *Biochim. Biophys. Acta 576*, 409–423.
Piantini, U., Sørensen, O. W., & Ernst, R. R. (1982) *J. Am. Chem. Soc. 104*, 6800–6801.
Rance, M., & Wright, P. E. (1986) *J. Magn. Reson. 66*, 372–378.
Segal, G. P., Lehrer, R. I., & Selsted, M. E. (1985) *J. Infect. Dis. 151*, 890–894.
Selsted, M. E., & Harwig, S. S. (1987) *Infect. Immun. 55*, 2281–2286.
Selsted, M. E., Szklarek, D., & Lehrer, R. I. (1984) *Infect. Immun. 45*, 150–154.
Selsted, M. E., Harwig, S. S., Ganz, T., Schilling, J. W., & Lehrer, R. I. (1985a) *J. Clin. Invest. 76*, 1436–1439.
Selsted, M. E., Brown, D. M., DeLange, R. J., Harwig, S. S., & Lehrer, R. I. (1985b) *J. Biol. Chem. 260*, 4579–4584.
Selsted, M. E., Szklarek, D., Ganz, T., & Lehrer, R. I. (1985c) *Infect. Immun. 49*, 202–206.
States, D. J., Haberkorn, R. A., & Ruben, D. J. (1982) *J. Magn. Reson. 48*, 286–292.
Wagner, G., & Wüthrich, K. (1982) *J. Mol. Biol. 160*, 343–361.
Wagner, G., Pardi, A., & Wüthrich, K. (1983) *J. Am. Chem. Soc. 105*, 5948–5949.
Wilde, C. G., Griffith, J. E., Marra, M. N., Snable, J. L., & Scott, R. W. (1989) *J. Biol. Chem. 264*, 11200–11203.
Williamson, M. P. (1990) *Biopolymers 29*, 1423–1431.
Wishart, D. S., Sykes, B. D., & Richards, F. M. (1991) *J. Mol. Biol. 222*, 311–333.
Wüthrich, K. (1986) *NMR of Proteins and Nucleic Acids*, John Wiley & Sons, New York.
Zhang, X. L. (1989) Ph.D. Thesis *Solution Structures of Antimicrobial Peptides Determined by Nuclear Magnetic Resonance Spectroscopy and Distance Geometry Techniques*, Rutgers University, New Brunswick, NJ.